A METHOD OF CALCULATING THE TRANSITION REGION FOR TWO-DIMENSIONAL BOUNDARY LAYERS WITH DISTRIBUTED SUCTION

by

J.L. van Ingen

Department of Aeronautical Engineering
Technological University Delft
The Netherlands

Paper presented at the 6th European Aeronautical Congress
Munich, Sept 1-4, 1965

Note: This publication is a summary of the transition related experimental and theoretical research that is discussed in detail in the next items on the CD-ROM, taken from the PhD thesis (1965) of the author. At this stage of the development the Pretsch charts had been reduced to an interpolation table with about 300 numbers.

A method of calculating the transition region for two-dimensional boundary layers with distributed suction

by

J.L. van Ingen

Department of Aeronautical Engineering
Technological University Delft
the Netherlands

july 1965

Paper to be presented at the 6th European Aeronautical Congress, Munich, sept. 1-4, 1965

A method of calculating the transition region for two-dimensional boundary layers with distributed suction.

Summary

The method uses linear stability theory to calculate the "amplification factor" σ_a of unstable disturbances in the laminar boundary layer. It is shown that at the experimentally determined transition position this factor σ_a has roughly the same value for different experiments with and without suction. Hence, in reverse the transition position can be calculated assuming that transition occurs as soon as σ_a has reached this critical value.
This work is an extension of an earlier method - valid for the no-suction case - which had been developed independently by Smith and the present author.

Sommaire

Une méthode à calculer la région de transition dans la couche limite laminaire avec aspiration poreuse.

La méthode emploie la théorie d'instabilité linéaire pour calculer "le coefficient d'amplification σ_a" des perturbations instabiles dans la couche limite laminaire. On montre que, pour le point de transition déterminé expérimentalement, ce coefficient atteint environ la meme valeur pour des expériences différentes avec et sans aspiration. En conséquence la position de transition peut etre calculé en supposant que transition commence dès que le coefficient σ_a a gagné cette valeur critique.
L'oeuvre présenté ici est une extension d'une méthode précédente - applicable à des cas sans aspiration - qui était développé indépendamment par Smith et I'auteur de cette note.

Zusammenfassung

Ein Verfahren zur Berechnung der Umschlagstelle der zweidimensionalen laminaren Grenzschicht mit kontinuierlicher Absaugung.

Das Verfahren benutzt die lineare Stabilitätstheorie zur Berechnung eines "Anfachungs faktors σ_a" der instabilen Störungen in die laminare Grenzschicht. Es wird gezeigt dass für die experimentell bestimmte Umschlagstelle, dieser Faktor σ_a für verschiedene Fälle mit und ohne Absaugung etwa derselben Wert

erreicht.

Darum kann, umgekehrt, die Umschlagstelle errechnet werden wenn man annimmt dass Umschlag beginnt sobald σ_a den Kritischen Wert erreicht.

Die heutige Arbeit ist eine Erweiterung eines früheren Verfahrens - anwendbar für Grenzschichten ohne Absaugung - das unabhängig von einander sowohl von Smith als von dem Verfasser dieses Berichtes entwickelt worden ist.

Contents

	page
1. List of symbols	5
2. Introduction	6
3. Principles of linear stability theory	8
3.1. General	8
3.2. The stability diagram	9
3.3. The amplification factor	10
3.4. Available stability diagrams	12
3.5. Some results of Pretsch' stability calculations for the Hartree velocity profiles	13
4. Some existing methods for the calculation of the transition point	14
5. A new method for the semi-empirical determination of the transition region	15
5.1. General	15
5.2. The amplification factor for the flat plate without suction	15
5.3. The amplification factor for the EC 1440 airfoil section without suction	17
5.4. Some results for the flat plate with constant suction velocity	18
5.5. Some results for the NACA 64_2-A-215 airfoil with suction	20
6. Conclusions	20
7. References	21
Tables 1 and 2	
Figures 1-12	

1. List of symbols.

c	reference length, equal to chord length for airfoil sections.
$\bar{c}$	$c_r + i\, c_i = \frac{\bar{\beta}}{\bar{\alpha}} = \frac{\beta_r}{\alpha} + i\,\frac{\beta_i}{\alpha}$
c_q	suction flow coefficient $\frac{Q}{U_\infty c}$ ($-v_o/U$ for flat plate with constant v_o)
f	number denoting value of reduced frequency $\frac{\beta_r \nu}{U^2}$ in table 2
K_1, K_2	constants in equation (10)
Q	suction flow per unit span
R_{δ^*}	$\frac{U\delta^*}{\nu}$
R_θ	$\frac{U\theta}{\nu}$
R_c	$\frac{U_\infty c}{\nu}$
s	distance along contour of airfoil section, measured from leading-edge
$\bar{s}$	s/c
t	time
T	amplification rate of unstable disturbances, defined by eq. 9
T_o	constant in equation (10)
u	velocity component parallel to wall
$\bar{u}$	u/U
U	velocity component parallel to wall at edge of boundary layer
$\bar{U}$	U/U_∞
U_∞	reference speed; equal to windspeed for figs 11 and 12
v_o	normal velocity at surface; negative for suction
x	distance along surface, measured from forward stagnation point
$\bar{x}$	x/c
y	distance normal to wall
α	angle of attack
$\bar{\alpha}$	$2\pi/\lambda$
β	Hartree parameter
$\bar{\beta}$	$\beta_r + i\beta_i$
δ^*	displacement thickness $\int_o^\infty (1-\bar{u})dy$

Θ	momentum loss thickness $\int_0^\infty \bar{u}(1-\bar{u})dy$
λ	wave length of disturbance
λ	Pohlhausen parameter
ν	coefficient of kinematic viscosity
σ_a	amplification factor defined by equation (8)
$\varphi(y)$	$\varphi_r + i\varphi_i$ amplitude function
ψ	$\psi_r + i\psi_i$ stream function of disturbance defined by equation (1)

subscripts

i	at instability point
o	at surface
tr	at transition

2. Introduction.

Although the phenomenon of transition has been known already since Reynolds' famous experiments on pipe flow in 1883 [8] the mechanism of transition is not yet completely understood. Neither is it possible to predict theoretically for an arbitrary body the position where transition will occur.

For a long time there have been two conflicting opinions about the mechanism of transition. One school of thought supposes that disturbances in the flow outside the boundary layer cause fluctuations inside the boundary layer which lead to local and instantaneous separation followed by transition (Taylor [9]).

A different explanation is given by the so called stability theory as developed by Rayleigh, Tollmien, Schlichting, Lin, etc. (see [7] chapter 16). In this theory it is shown that small harmonic disturbances in the boundary layer may become unstable and amplify. It is supposed that these disturbances cause transition as soon as they have gained a sufficient amplification.

The unstable oscillations, predicted by the stability theory were discovered in wind tunnel experiments on the boundary layer of a flat plate by Schubauer and Skramstad in 1940 [10]. It was found that the stability theory is valid only if the degree of turbulence in the airstream is less than $0.1^{o}/o$. For high turbulence levels Taylor's theory is more appropriate. In 1951 the existence of unstable oscillations was also shown in free flight by Malotaux et al [11]. In the free atmosphere and in modern low speed wind tunnels the degree of turbulence is considerably less than $0.1^{o}/o$ and it is commonly accepted

now that under these circumstances transition on smooth bodies - at least initially - is governed by the stability theory. An exception should be made for cases where the laminar boundary layer separates from the surface due to an adverse pressure gradient. It may be possible that a short distance upstream of the imminent separation Taylor's transition mechanism is the relevant one. Also transition in the separated layer may be governed by a different mechanism.

Stability theory shows under which circumstances the laminar boundary layer may become unstable and predicts the initial growth of the disturbances. Since most of the existing theories are linearised by assuming small disturbances they cannot describe the complete transition to the irregular turbulent flow with relatively large disturbances.

Our knowledge of transition has been steadily enlarged however through experiments, starting with the well known investigations by Schubauer and Skramstad. A review of this work may be found in [7]. Some recent results have been described by Hinze et al. [12].

From the experiments it is known that in the transition region suddenly "turbulent spots" are generated. These spots grow and merge as they move downstream until finally at a certain position the flow is fully turbulent [13,14]. According to Klebanoff and Tidstrom [15] the spots seem to develop from threedimensional concentrations of disturbance energy in the originally two-dimensional disturbance waves.

For the prediction of the aerodynamic characteristics of airfoil sections it is necessary to possess a method to calculate the transition position of the boundary layer. Since the transition process is not yet sufficiently understood theoretically such a method will necessarily be a semi-empirical one.

A method of this type has been developed for boundary layers without suction by Smith and Gamberoni [1,2] and independently by the present author [3,4,5]. The method is based on the linear stability theory; in the first few sections of this paper the principal results of this theory will be collected for later use. In the final sections the method for the calculation of the transition position will be described. It will be shown that the method is also applicable in the case of suction through a porous surface.

Throughout the present work it will be assumed that the boundary layer flow is two-dimensional and incompressible; the influence of surface roughness on transition will not be considered.

For all boundary layer calculations in the present work a Pohlhausen-type method has been used which was developed by the author. A description of this method and also a more detailed review of the present work may be found in [6].

3. Principles of linear stability theory.

3.1. General.

The stability theory considers a given laminar main flow upon which small disturbances are superimposed. It is assumed that both the undisturbed and the disturbed flow satisfy the Navier-Stokes equations. After linearisation the well known Orr-Sommerfeld equation is obtained which under certain circumstances may possess unstable solutions. It is found that important factors determining the stability or instability are

the shape of the boundary layer velocity profile
the Reynoldsnumber $\frac{U\delta^*}{\nu}$ or $\frac{U\theta}{\nu}$
and the frequency or wavelength of the disturbances.

In the theory a two-dimensional periodic disturbance is assumed with a stream function ψ defined by

$$\psi(x,y,t) = \varphi(y)\, e^{i(\bar{\alpha}x - \bar{\beta}t)} \qquad (1)$$

In (1) it is assumed that $\bar{\alpha}$ is a real quantity; it determines the wave length λ of the disturbance by $\lambda = 2\pi/\bar{\alpha}$; $\bar{\beta}$ is complex with $\bar{\beta} = \beta_r + i\beta_i$ where $\beta_r/2\pi$ is the frequency of the disturbance. The sign of β_i determines whether the disturbance is stable or unstable. For stable or unstable disturbances β_i is negative or positive respectively; neutrally stable disturbances correspond to $\beta_i = 0$. The amplitude function $\varphi(y)$ is complex and is assumed to depend on y only.

Furthermore use will be made of

$$\bar{c} = c_r + ic_i = \frac{\beta_r}{\bar{\alpha}} + i\,\frac{\beta_i}{\bar{\alpha}} \qquad (2)$$

the sign of c_i again determines the stability of the disturbance; c_r is the wave speed.

Possible non-zero solutions of the Orr-Sommerfeld disturbance equation are found by solving an eigen-value problem. This will not be pursued further in the present paper; extensive reviews may be found in [7,16].

In the following sections only those results of stability theory will be presented which are used in the remainder of the present paper.

3.2. The stability diagram.

For a given laminar boundary layer $\frac{U\delta^*}{\nu}$ and the shape of the velocity profile are known. Then in the stability problem $\bar{\alpha}\delta^*$, c_r/U and c_i/U remain as parameters. Usually c_r/U and c_i/U are replaced by $\frac{\beta_r \nu}{U^2}$ and $\frac{\beta_i \delta^*}{U}$ using the following expressions:

$$\frac{c_r}{U} = \frac{\beta_r \nu}{U^2} \cdot \frac{1}{\bar{\alpha}\delta^*} \cdot \frac{U\delta^*}{\nu}$$

and

$$\frac{c_i}{U} = \frac{\beta_i \delta^*}{U} \cdot \frac{1}{\bar{\alpha}\delta^*}$$

Now, when a value for one of these parameters is assumed (for instance $\bar{\alpha}\delta^*$) the values of the other ones may be determined for which the Orr-Sommerfeld equation allows non-zero solutions. Results of these calculations are usually presented in an $\bar{\alpha}\delta^*$ - $\frac{U\delta^*}{\nu}$ plane: the "stability diagram". The curve for $\frac{\beta_i \delta^*}{U} = 0$ denotes the neutrally stable disturbances. Inside the loop β_i is positive and outside negative. This means that unstable disturbances will be found only for combinations of $\bar{\alpha}\delta^*$ and $\frac{U\delta^*}{\nu}$ inside the loop. Below a certain value of $\frac{U\delta^*}{\nu}$ there are no values of $\bar{\alpha}\delta^*$ for which unstable disturbances are possible; this value of $\frac{U\delta^*}{\nu}$ is called the critical Reynoldsnumber.

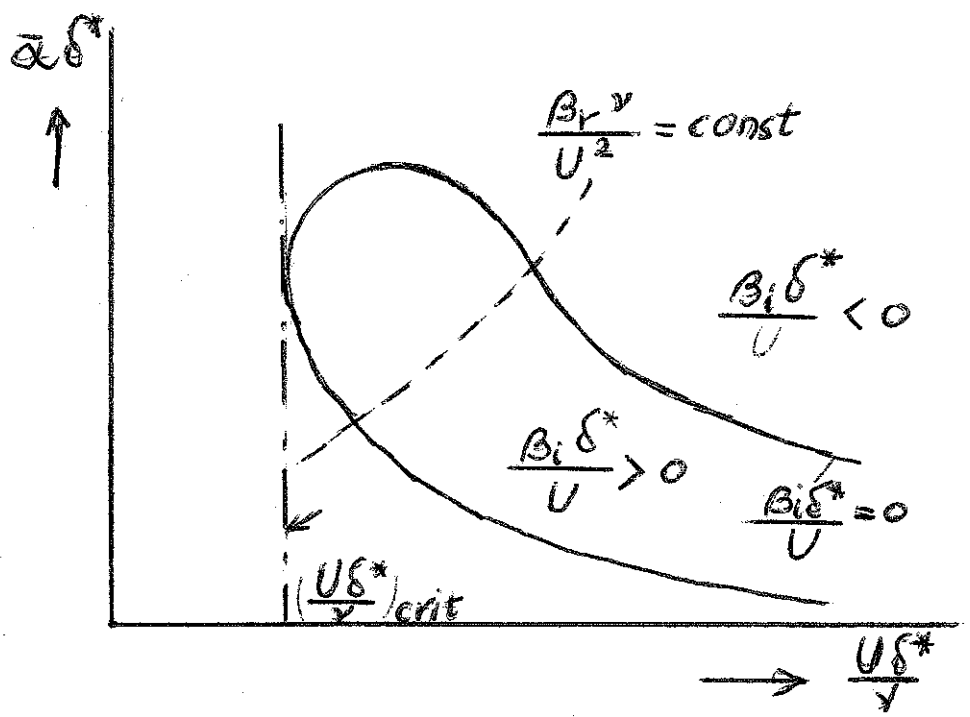

The stability diagram, as discussed here, is only valid for parallel flows

where the velocity profile and $\frac{U\delta^*}{\nu}$ do not change with x. It is general practice to apply results of stability calculations also to flows where u(y) changes slowly with x. This implies that at each station x the actual flow is replaced by a parallel flow with the same non-dimensional velocity profile $\bar{u}(y/\delta^*)$ and Reynoldsnumber $\frac{U\delta^*}{\nu}$. For a similar boundary layer the shape of the non-dimensional velocity profile is independent of x and hence the same stability diagram applies at all values of x. If now a disturbance with a constant value of $\frac{\beta_r \nu}{U^2}$ is considered which is convected downstream with the flow, it follows - because $\frac{U\delta^*}{\nu}$ increases with x - that the disturbance may at first be stable, then become unstable and finally become stable again. The same happens for non-similar boundary layers where however the stability diagram changes with x.

The stability diagram is found to depend on the shape of the velocity profile. It turns out that the curvature of the profile is very important: profiles with a point of inflexion have a much lower critical Reynoldsnumber and hence are much less stable than velocity profiles without inflexion point. Hence it follows that factors determining the occurrence of an inflexion point have much influence on stability and hence on transition.

An inflexion point occurs if $\frac{\partial^2 u}{\partial y^2}$ at the wall is positive. From the boundary layer equations it follows easily that $(\frac{\partial^2 u}{\partial y^2})_o$ depends on the pressure gradient term $U \frac{dU}{dx}$ and the suction velocity v_o. An "adverse" pressure gradient ($\frac{dU}{dx} < 0$) or blowing ($v_o > 0$) tend to make $(\frac{\partial^2 u}{\partial y^2})_o > 0$ and hence are destabilising factors. A "favourable" pressure gradient ($\frac{dU}{dx} > 0$) or suction ($v_o < 0$) tend to make $(\frac{\partial^2 u}{\partial y^2})_o < 0$ and hence are stabilising factors.

3.3. The amplification factor.

It was mentioned in section 3.1 that the amplification or damping of disturbances in the boundary layer is determined by the magnitude of β_i. In what follows an equation will be derived which governs the growth of the amplitude of the disturbances. This equation follows from the expression (1) for the stream function. Of course, only the real part of the stream function ψ_r is physically significant.

From equation (1) together with $\varphi = \varphi_r + i\varphi_i$ it follows that

$$\psi_r = e^{\beta_i t} \left[\varphi_r \cos(\bar{\alpha}x - \beta_r t) - \varphi_i \sin(\bar{\alpha}x - \beta_r t) \right]$$

or denoting $\frac{\varphi_r}{\varphi_i}$ by tg γ

$$\psi_r = -e^{\beta_i t} \frac{\varphi_i}{\cos \gamma} \sin (\bar{\alpha}x - \beta_r t - \gamma) \tag{3}$$

For the velocity components u' and v' of the disturbance similar expressions are found. Because φ and hence γ depend only on y the amplitudes a and a + da for a fixed value of y at times t and t + dt are related by

$$d(\ln a) = \beta_i \, dt \tag{4}$$

Hence if the amplitude for the neutral oscillation at time t_o is denoted by a_o, the amplitude at a later time t follows from

$$\ln \frac{a}{a_o} = \int_{t_o}^{t} \beta_i \, dt \tag{5}$$

or $$\frac{a}{a_o} = e^{\sigma_a} \quad \text{where} \quad \sigma_a = \int_{t_o}^{t} \beta_i \, dt \tag{6}$$

In what follows σ_a will be called the "amplification factor".
For parallel flows the parameter β_i in (6) is constant but it may vary with x for non-parallel flow.
Since the integration variable t in (6) is somewhat obscure for stability calculations in boundary layers a change will be made to the variable x by using

$$\frac{dx}{dt} = c_r \tag{7}$$

This means that a disturbance is followed on its way downstream. Using (7) equation (6) for σ_a may be written as

$$\sigma_a = \int_{x_o}^{x} \frac{\beta_i}{c_r} \, dx$$

or after introducing convenient non-dimensional quantities

$$\sigma_a = \frac{U_\infty c}{\nu} \cdot 10^{-6} \int_{\bar{x}_o}^{\bar{x}} T.\bar{U} \, d\bar{x} \tag{8}$$

In equation (8) T denotes

$$T = \frac{\frac{\beta_i \delta^*}{U} \cdot \bar{\alpha}\delta^* . 10^6}{\frac{\beta_r \nu}{U^2} \cdot \left(\frac{U\delta^*}{\nu}\right)^2} \qquad (9)$$

and $\bar{x} = \frac{x}{c}$ where c is a constant reference length. The quantity T may be calculated as a function of $\bar{x}$ for a given value of $\frac{\beta_r \nu}{U^2}$ if the shape of the velocity profile and $\frac{U\delta^*}{\nu}$ are known as functions of $\bar{x}$. Moreover stability diagrams have to be known for the velocity profiles encountered.
The lower integration limit $\bar{x}_o$ in (8) denotes the value of $\bar{x}$ at which for the frequency considered $\frac{\beta_i \delta^*}{U} = 0$ for the first time.

3.4. Available stability diagrams.

Since the stability calculations are rather laborious not many stability diagrams have been calculated. A review of these results may be found in [7], chapter 16 and [16], a selection of these results has been given in [6].
For the flat plate boundary layer without suction critical Reynoldsnumbers from different sources have been collected in table 1. It may be seen that the results of various calculations show considerable differences. This is caused on the one hand by the different procedure followed for the stability calculations. On the other hand the Blasius profile has been approximated by different analytical expressions; in many cases the velocity profile for the flat plate boundary layer from some Pohlhausen type method has been used. Since these velocity profiles and especially their curvature may be different, the stability diagrams are not necessarily identical.
Calculations for a series of Hartree velocity profiles have been made by Pretsch [17-19]; these results will be discussed in more detail in section 3.5.
A comparison of results obtained from different sources (see [6]) shows that the stability diagrams calculated by the same author for different boundary layers, at equal values of the critical Reynoldsnumber, do not differ more than those obtained by different authors for the same flow.
In the remainder of the present work the amplification factor for boundary layers with arbitrary pressure- and suction distributions will be calculated. For this calculation stability diagrams including information about the amplification rate at $\beta_i > 0$ have to be known. To the best of the author's

knowledge these results are only provided by Pretsch's stability diagrams and it will be attempted to apply these diagrams to arbitrary boundary layers. In view of the comparisons of different stability diagrams mentioned above, the following procedure seems to be justified for assigning a stability diagram to a certain velocity profile. From an approximate formula due to Lin [16] the critical Reynoldsnumber is found. Then the stability diagram from Pretsch's series with the same critical Reynolds number is assumed to be valid for the velocity profile under investigation. This implies that all stability diagrams are considered to form a one-parameter family with the critical Reynoldsnumber as parameter. Since in boundary layer calculations using the von Kármán momentum equation the momentum loss thickness Θ is the proper thickness parameter it is advantageous to use a Reynoldsnumber based on Θ. This will be done in what follows.

3.5. Some results of Pretsch' stability calculations for the Hartree velocity profiles.

Detailed stability calculations for some of the Hartree profiles have been made by Pretsch. Some additional stability diagrams have been obtained by Smith and Gamberoni [1] from interpolation in Pretsch results. In what follows these diagrams will be used to calculate the amplification factor σ_a. It may be seen from equation (8) that the only information needed from the diagrams is the quantity T as defined by equation (9). Values of T for a range of values of $\frac{\beta_r \nu}{U^2}$ and $\frac{U\delta^*}{\nu}$ have been obtained from Pretsch' work for β = 1, 0.6, 0, -0.10, -0.198 and for β = 0.2, 0.1, -0.05 from [1]; (β denotes the well known shape parameter of the Hartree profiles).

In fig. 1 for example the results are shown for the flat plate (β=0) plotted as function of $^{10}\log \frac{U\Theta}{\nu}$. It is seen from the figure that the curves for constant values of $\frac{\beta_r \nu}{U^2}$ may be approximated by parabola's of the form

$$T = T_o - K_1 \left(^{10}\log \frac{U\Theta}{\nu} - K_2\right)^2 \qquad (10)$$

where the coefficients T_o, K_1 and K_2 depend on β and $\frac{\beta_r \nu}{U^2}$. Values for these coefficients have been obtained for all values of β and a range of values for $\frac{\beta_r \nu}{U^2}$. The approximation given by (10) to the actual values is shown in fig. 1.

Finally cross plots have been made to find T_o, K_1 and K_2 as functions of β for constant values of $\frac{\beta_r \nu}{U^2}$. Since a unique relation exists between β and $(\frac{U\Theta}{\nu})_{crit}$

it is possible to consider T_o, K_1 and K_2 as functions of $^{10}\log\left(\frac{U\theta}{\nu}\right)_{crit}$.
Since it may be expected that Pretsch's results will not be very accurate, linear interpolation in $^{10}\log\left(\frac{U\theta}{\nu}\right)_{crit}$ seems to be justified to find the coefficients of (10) for arbitrary values of $^{10}\log\left(\frac{U\theta}{\nu}\right)_{crit}$. Table 2 gives T_o, K_1 and K_2 for different values of $\frac{\beta_r \nu}{U^2}$ at equidistant values of $^{10}\log\left(\frac{U\theta}{\nu}\right)_{crit}$. The numbers quoted in the table have been chosen in such a way that by linear interpolation in $^{10}\log\left(\frac{U\theta}{\nu}\right)_{crit}$ the values obtained from Pretsch's diagrams will be regained.
For convenience the reduced frequencies $\frac{\beta_r \nu}{U^2}$ have been denoted by a number f in table 2; results for intermediate values of $\frac{\beta_r \nu}{U^2}$ can be obtained by linear interpolation in the parameter f.
In what follows it will be assumed that table 2 can be applied to boundary layer flows with arbitrary suction- and pressure distributions.

4. Some existing methods for the calculation of the transition point.

In preceding sections it has been shown that it is possible to determine theoretically whether a particular boundary layer flow is stable or unstable. For instance for the flat plate the boundary layer becomes unstable as soon as $\frac{U\delta^*}{\nu}$ exceeds a critical value of about 575 corresponding to $\frac{Ux}{\nu} = 0.11 \times 10^6$. From experiments it is known however that actual transition starts at $\frac{Ux}{\nu} = 2.8 \times 10^6$ only. This means that a considerable distance will exist between the point of instability and the transition point.
Since the transition process is not sufficiently understood theoretically it is only possible to calculate the transition position by using semi-empirical methods. Some of these methods are mentioned below.

In some methods the results of different transition measurements are plotted in such a way that all points fall - as far as possible - on a single curve. For a new case transition may be "predicted" by assuming that the new case will also fall on this universal curve. An important example of these methods is due to Michel [20]. In his method $\frac{U\theta}{\nu}$ at the transition point is plotted versus the corresponding value of $\frac{Ux}{\nu}$; indeed results of different experiments fall reasonably well on a single curve. The method is based on experiments without suction and can not easily be generalised to suction problems.

A different method has been given by Granville [21]. Here a universal curve is obtained by plotting $(\frac{U\theta}{\nu})_{tr} - (\frac{U\theta}{\nu})_{i}$ versus the mean value $\overline{\Lambda_1}$ of the Pohlhausen parameter $\Lambda_1 = \frac{\theta^2}{\nu}\frac{dU}{dx}$ defined by

$$\overline{\Lambda_1} = \frac{1}{\bar{x}_{tr} - \bar{x}_i} \int_{\bar{x}_i}^{\bar{x}_{tr}} \Lambda_1 \, d\bar{x} \qquad (11)$$

The subscripts "tr" and "i" denote transition and instability respectively. Another suggested method is to assume that transition occurs at a constant value of $\frac{U\delta^*}{\nu}$. This results in a very rough estimate of the transition point only.

To improve upon the above methods the determination of the transition point should not be based on local quantities only but the history of the boundary layer should be taken into account, because this determines the amplification of unstable disturbances. Such a method will be presented in the next section.

5. A new method for the semi-empirical determination of the transition region.

5.1. General.

It was shown by Smith and Gamberoni [1,2] and at the same time independently by the present author [3,4,5] that different experiments on transition without suction can be correlated on the basis of the amplification factor σ_a. It was shown that the maximum value of σ_a which was reached at the transition position was roughly equal for all cases investigated. Hence in new cases an accurate estimate of the transition position may be found using the assumption that transition occurs as soon as the calculated value of $(\sigma_a)_{max}$ reaches this critical value. In the references cited above the method was shown to be valid for the no-suction case. It will be presented here in a modified form; furthermore it will be shown that the method is also applicable to cases with suction.

5.2. The amplification factor for the flat plate without suction.

The amplification factor σ_a is defined by equation (8)

$$\sigma_a = 10^{-6} \frac{U_\infty c}{\nu} \int_{\bar{x}_o}^{\bar{x}} T.\bar{U} \, d\bar{x} \qquad (12)$$

If for the flat plate the reference velocity U_∞ and the reference length c are chosen as U and $\frac{\nu}{U}$ respectively, equation (12) reduces to

$$\sigma_a = 10^{-6} \int_{\frac{Ux_o}{\nu}}^{\frac{Ux}{\nu}} T \, d\left(\frac{Ux}{\nu}\right) \qquad (13)$$

For the flat plate the relation between $\frac{U\theta}{\nu}$ and $\frac{Ux}{\nu}$ is known and it is possible to calculate σ_a for different frequencies $\frac{\beta_r \nu}{U^2}$ using table 2 and the formulae given in section 3.5. For this calculation a value of $\left(\frac{U\theta}{\nu}\right)_{crit}$ has to be assumed; as some uncertainty exists here (see table 1) a range of values for the critical Reynoldsnumber has been used. For $\left(\frac{U\theta}{\nu}\right)_{crit} = 260$, which is the value obtained by Pretsch for $\beta = 0$, some results are shown in figs 2 and 3. Values of T are shown in fig. 2; the amplification factor σ_a is shown in fig. 3 where also the envelope giving the maximum amplification factor $(\sigma_a)_{max}$ has been drawn.

Similar calculations have been performed for other values of $\left(\frac{U\theta}{\nu}\right)_{crit}$ from table 1; the results for $(\sigma_a)_{max}$ have been collected in fig. 4.

Of course the calculation of the amplification factor can be extended to arbitrary high Reynoldsnumbers. However, it is known from experiments (Schubauer and Skramstad [10]) that transition sets in at $\frac{Ux}{\nu} = 2.8 \times 10^6$ and that the boundary layer is completely turbulent for $\frac{Ux}{\nu} > 3.9 \times 10^6$. These limits have been inserted in fig. 4, it follows that to these values of $\frac{Ux}{\nu}$ certain values of $(\sigma_a)_{max}$ correspond.

If Pretsch's value is used it is found that beginning and end of the experimentally determined transition region correspond to $(\sigma_a)_{max} = 7.6$ and 9.7 respectively. In the earlier version of the method [3,4,5] the values 7.8 and 10 were obtained. The slight differences with the present values are easily explained by the fact that at that time only small scale versions of Pretsch's charts were available to the author which could not be read very accurately.

In the further calculations the method of [6] will be used in combination with Lin's formulae for the critical Reynoldsnumber. Table 1 and fig. 5 show that this leads to $(\sigma_a)_{max} = 9.2$ and 11.2 at the beginning and end of the transition region respectively. In what follows it will be shown that nearly the same values are obtained for other boundary layers. It should be noted that the

linear stability theory has been used to calculate σ_a up till transition but of course not too much significance should be attached to the details of these calculations. The maximum amplification factor has to be considered only as a convenient parameter correlating different factors which influence the transition.

5.3. The amplification factor for the EC 1440 airfoil section without suction.

For airfoil sections the boundary layer is not similar and hence for different values of $\bar{x}$ different stability diagrams have to be used. If $(\frac{U\theta}{\nu})_{crit}$ is known as a function of $\bar{x}$, for instance from Lin's formulae, it is easily possible to calculate σ_a also for these cases using table 2.

In [3,4,5] results of transition measurements and calculations of the amplification factor for the EC 1440 airfoil section have been presented. In this work Pohlhausen's method was used for the boundary layer calculations; critical Reynoldsnumbers for the velocity profiles were found by relating Pohlhausen's λ to Hartree's β used by Pretsch. This relation was obtained by calculating the Hartree boundary layers for $U = u_1 x^{\frac{\beta}{2-\beta}}$ with Pohlhausen's method. The examples discussed in [3,4,5] will be recalculated here using the method of [6] in combination with Lin's formulae. Results of the amplification calculation for $\alpha = 0$ are shown in figs 5 and 6. Similar calculations have been performed for other values of α; the results have been used to construct fig. 7 where also the experimentally determined transition region is shown. The curve $(\sigma_a)_{max} = 0$ in fig. 7 denotes the instability point; it follows that both the instability point and transition move forward with increasing angle of attack.

However, the distance between the instability point and transition can be very large. If the beginning of transition is assumed to occur for $(\sigma_a)_{max} = 9.2$ it may be seen from fig. 7 that the beginning of transition is predicted accurately within $5^o/o$ of the chord length for $\alpha > -2^o$.

For $\alpha < -2^o$ transition is preceded by laminar separation; in this case the distance between the predicted and actual positions wheretransition starts may grow to $10^o/o$ of the chord length.

Smith and Gamberoni [1,2] applied a similar analysis to a great number of experimental data including results of free flight measurements. They calculated the laminar boundary layer by means of a method which for the flat plate produces Hartree's velocity profile for $\beta = 0$. Hence, using Pretsch' value

for the critical Reynoldsnumber they should find $(\sigma_a)_{max} = 7.6$ and 9.7 at the beginning and end of the transition region. The conclusion of their analysis was that $(\sigma_a)_{max} = 9$ would correlate the experimental data very well. Since no distinction was made between beginning and end of the transition region the agreement with the values 7.6 and 9.7 is very good. A difference between the present method and the method of Smith and Gamberoni is that the last authors calculate the amplification at constant values of $\frac{\beta_r \nu}{U_\infty^2}$ while for the present method constant values of $\frac{\beta_r \nu}{U^2}$ are used. Since $\overline{U} = U/U_\infty$ does not change very much in the regions of interest and moreover only the envelope of σ_a for different frequencies is used this difference apparently has no effect on the results.

Anticipating the results of an experimental investigation on the effects of suction through a porous surface - to be discussed in section 5.5 - it is stated here already that the method is also applicable in the case of suction.

5.4. Some results for the flat plate with constant suction velocity.

The boundary layer on a flat plate with constant suction velocity has been discussed by Iglisch [22]. It was found that the non-dimensional parameter $\Lambda_2 = \frac{-v_o \Theta}{\nu}$ and the shape of the velocity profile only depend on the variable $\overline{x}$ defined by

$$\overline{x} = \left(\frac{-v_o}{U}\right)^2 \frac{Ux}{\nu} \tag{14}$$

Since the critical Reynoldsnumber depends on the shape of the velocity profile only it also depends only on $\overline{x}$.

Values of $\frac{U\Theta}{\nu}$ may be found as function of $\overline{x}$ for different values of the suction coefficient $c_q = \frac{-v_o}{U}$ from

$$\frac{U\Theta}{\nu} = \frac{\frac{-v_o \Theta}{\nu}}{\frac{-v_o}{U}} \tag{15}$$

Results of some calculations using the method of G: in combination with Lin's formulae for the critical Reynoldsnumber, are shown in fig. 8. It follows that for $\frac{-v_o}{U} \geq 0.980 \times 10^{-4}$ nowhere along the length of the plate $\frac{U\Theta}{\nu}$ will

exceed $(\frac{U\theta}{\nu})_{crit.}$ and hence the boundary layer is stable at all values of $\bar{x}$. For values of $\frac{-v_o}{U}$ less than 0.980×10^{-4} the boundary layer becomes unstable in a certain interval.

A similar calculation has been made by Ulrich [23] using Iglisch' exact solution for $\frac{U\theta}{\nu}$ and his own results for $(\frac{U\theta}{\nu})_{crit}$. He found that the suction coefficient c_q should exceed the value 1.18×10^{-4} to ensure a stable boundary layer for all values of $\bar{x}$. The difference between the values 1.18 and 0.980 is easily explained by the different procedures used to determine the critical Reynoldsnumber.

For the case of a constant suction velocity the amplification factor can easily be calculated as follows.

If the definition (14) for $\bar{x}$ is used it is implied that the reference length c has been defined as

$$c = \frac{U\nu}{(-v_o)^2} \tag{16}$$

If the reference speed U_∞ is made equal to the constant free stream speed U then the Reynoldsnumber $R_c = \frac{U_\infty c}{\nu}$ becomes

$$R_c = \left(\frac{U}{-v_o}\right)^2 = c_q^{-2} \tag{17}$$

and equation (8) reduces to

$$\sigma_a = 10^{-6}\, c_q^{-2} \int_{\bar{x}_o}^{\bar{x}} T\, d\bar{x} \tag{18}$$

Results of amplification calculations for different values of c_q have been collected in fig. 9 where $(\sigma_a)_{max}$ is shown as function of $\bar{x}$. The peak value of the amplification factor is plotted in fig. 10 as function of c_q. If it is assumed that transition starts as soon as $(\sigma_a)_{max}$ reaches the critical value 9.2, then it may be concluded from fig. 10 that transition will not occur unless c_q falls below the value 0.485×10^{-4}. This value is only 50°/o of the suction coefficient required to keep the boundary layer stable.

5.5. Some results for the NACA 64_2-A-215 airfoil with suction.

Some investigations have been made on the NACA 64_2-A-215 airfoil with suction through a porous surface between the 30^{o}/o and 90^{o}/o chord positions. An extensive review of this work may be found in [6]; in the present paper only a few typical results will be presented.

Figs. 11 and 12 show a comparison between the calculated and measured transition position for the upper surface at different values of the suction flow coefficient c_q. It may be seen that the rearward movement of transition due to suction is predicted rather accurately.

6. Conclusions.

It has been shown that an earlier method for the prediction of transition for two-dimensional boundary layers without suction is also applicable in the case of suction through a porous surface. Using this method it becomes possible to design rational suction distributions for a given airfoil or to improve the design of the airfoil section itself.

7. References.

1. Smith, A.M.O., Gamberoni, N.: Transition, pressure gradient, and stability theory. Report ES 26388, Douglas Aircraft Co, 1956.
2. Smith, A.M.O.: Transition, pressure gradient and stability theory. Proc. 9th Int. Congr. Appl. Mech., Brussels, 4, p 234-244, 1956.
3. Ingen, J.L. van: Een semi-empirische methode voor de bepaling van de ligging van het omslaggebied van de grenslaag bij onsamendrukbare tweedimensionale stromingen (in Dutch). Rept VTH-71, Dept. Aeron. Eng. Delft 1956.
4. Ingen, J.L. van: A suggested semi-empirical method for the calculation of the boundary layer transition region. Rept VTH-74, Dept. Aeron. Eng., Delft, 1956.
5. Ingen, J.L. van: (same title as 4);Proc. Second European Aeron. Congr., Scheveningen, Netherlands 1956.
6. Ingen, J.L. van: Theoretical and experimental investigations of incompressible laminar boundary layers with and without suction. Rept. VTH-124; Dept. Aeron. Eng.; Delft 1965.
7. Schlichting, H.: Grenzschichttheorie. G.Braun, Karlsruhe, third edition, 1958. (see also Boundary layer theory, English edition, Pergamon Press, London, 1955).
8. Reynolds, O.: An experimental investigation of the circumstances which determine whether the motion of water shall be direct or sinuous, and of the law of resistance in parallel channels. Phil. Trans. 174, p 935-982, 1883.
9. Taylor, G.I.: Statistical theory of turbulence. V. Effect of turbulence on boundary layer. Proc. Roy. Soc. London, ser. A, vol 156, no 888, 1936, p 307-317.
10. Schubauer, G.B., Skramstad, H.K. Laminar boundary layer oscillations and transition on a flat plate. N.A.C.A. Rept 909, 1947.
11. Malotaux, P.C.A. et. al.: A method for qualitative boundary layer investigations by means of hot-wires without disturbing the flow. Rept. VTH-45, Dept. Aeron. Eng., Delft, 1951 (in Dutch with English summary).
12. Hinze, J.O. Contribution a la transition dans la couche limite. Compt. Rend. 8emes Journées de l'Hydraulique. Société Hydrotechnique de France, Lille, 1964.
13. Schubauer, G.B., Klebanoff, P.S.: Contributions on the mechanics of boundary layer transition. Proc. Symp. boundary layer effects in Aerodyn. N.P.L. 1955.
14. Schubauer, G.B.: Mechanism of transition at subsonic speeds. Proc. Symp. Boundary Layer Research, Int. Union theoret. appl. Mech. Freiburg p 85-109, 1957.

15. Klebanoff, P.S., Tidstrom, K.D.: The evolution of amplified waves leading to transition in a boundary layer with zero pressure gradient. N.A.C.A. T.N. D-195, 1959.

16. Lin, C.C.: The theory of hydrodynamic stability. Cambridge University Press, 1955.

17. Pretsch, J.: Die Stabilität einer ebenen Laminarströmung bei Druckgefälle und Druckanstieg. Jb. dtsch. Luftfahrt forsch. 1, p 158-75, 1941.

18. Pretsch, J.: Die Anfachung instabiler Störungen in einer laminaren Reibungsschicht. Jb. dtsch. Luftfahrtf. p 154-171, 1942.

19. Pretsch, J.: Berechnung der Stabilitätsgrenze von Grenzschichtprofilen und der Anfachung von Störungen. Göttinger Monograph. Part B.3.2. 1945.

20. Michel, R.: Détermination du point de transition et calcul de la trainée des profils d'ailes en incompressible. O.N.E.R.A. rept no 58, 1952.

21. Granville, P.S. The calculation of viscous drag of bodies of revolution. David Taylor Model Basin, Rept 849, 1953.

22. Iglisch, R.: Exakte Berechnung der laminaren Grenzschicht an der längsamgeströmten ebenen Platte mit homogener Absaugung. Schr. dtsch. Akad. Luftfahrtf. 8B, p1-51. (see also N.A.C.A. T.M. 1205).

23. Ulrich, A.: Theoretische Untersuchungen über die Widerstandsersparnis durch Laminarhaltung mit Absaugung. Schr. dtsch. Akad. Luftfahrtf. 8B, p53. (see also N.A.C.A. TM 1121).

24. Tollmien, W.: Über die Entstehung der Turbulenz. 1. Mitteilung, Nachr., Ges. Wiss. Göttingen, Math. Phys. Klasse, 21-44, 1929 (also NACA TM 609, 1931.)

25. Schlichting, H. and Ulrich, A.: Zur Berechnung des Umschlages laminar-turbulent Jahrbuch d. dt. Luftfahrtforschung I, 8, 1942.

26. Lin, C.C.: On the stability of two-dimensional parallel flows. Quarterly Appl. Math. Vol 3, july 1945, p 117-142; Vol 3, oct 1945, p 218-234; Vol 3, jan. 1946, p 277-301.

27. Shen, S.F. Calculated amplified oscillations in plane Poiseuille and Blasius flows. J. Aero. Sci. 21, p 62-64, 1954.

28. Timman, R., Zaat, J.A., Burgerhout, Th.J.: Stability diagrams for laminar boundary layer flow. N.L.L. Rept F 193, 1956.

Table 1: Critical Reynoldsnumber for the flat plate boundary layer.

$\frac{U\delta^*}{\nu}_{crit}$	$\frac{U\theta}{\nu}_{crit}$	$10_{\log}\left\{\frac{U\theta}{\nu}\right\}_{crit}$	references
321	124	2.093	Timman et. al. [28]
420	162	2.210	Tollmien [24]
420	162	2.210	Lin [26]
480	185	2.268	Lin, approximate formulae
575	222	2.346	Ulrich [23]
645	249	2.396	Schlichting-Ulrich [25]
680	260	2.416	Pretsch, $\beta = 0$ [17]
577	221	2.345	method of [6] with Lin's formulae

$10 \log \frac{U\theta}{\nu}_{crit}$	f = 1 $\frac{\beta_r \nu}{U^2} = 10^{-6}$			f = 2 $\frac{\beta_r \nu}{U^2} = 2.5\ 10^{-6}$			f = 3 $\frac{\beta_r \nu}{U^2} = 5.10^{-6}$		
	T_o	K_1	K_2	T_o	K_1	K_2	T_o	K_1	K_2
1	0.04	6.0	4.270	13.05	116.0	3.750	25.60	169	3.115
1.5	0.75	0	4.200	8.00	87.0	3.670	15.10	136	3.250
2	1.20	10.5	3.988	2.95	58.0	3.590	4.60	105	3.385
2.5	0.55	10.5	3.800	0.81	21.5	3.578	1.10	35	3.390
3	0.22	10.5	3.900	0.40	21.5	3.640	0.80	35	3.450
3.5	0.22	10.5	4.000	0.23	30.0	3.731	0	35	3.510
4	0.22	16.0	4.100	-0.22	38.5	3.825	0.80	35	3.570

$10 \log \frac{U\theta}{\nu}_{crit}$	f = 4 $\frac{\beta_r \nu}{U^2} = 7.5\ 10^{-6}$			f = 5 $\frac{\beta_r \nu}{U^2} = 10^{-5}$			f = 6 $\frac{\beta_r \nu}{U^2} = 2.5\ 10^{-5}$		
	T_o	K_1	K_2	T_o	K_1	K_2	T_o	K_1	K_2
1	33.80	212	3.020	39.90	245	2.966	62.70	401	2.790
1.5	19.70	180	3.140	23.10	213	3.068	36.60	365.5	2.845
2	5.60	148.5	3.260	6.30	181	3.170	10.50	331	2.900
2.5	1.55	54	3.270	2.15	76	3.200	3.90	196	2.945
3	1.10	44	3.338	1.10	54	3.260	-0.10	51.5	3.030
3.5	-0.275	44	3.402	-0.735	33	3.315	-4.10	0	3.113
4	-1.10	44	3.466	-2.40	11	3.370	-8.10	0	3.196

$10 \log \frac{U\theta}{\nu}_{crit}$	f = 7 $\frac{\beta_r \nu}{U^2} = 5.10^{-5}$			f = 8 $\frac{\beta_r \nu}{U^2} = 7.5\ 10^{-5}$			f = 9 $\frac{\beta_r \nu}{U^2} = 10^{-4}$		
	T_o	K_1	K_2	T_o	K_1	K_2	T_o	K_1	K_2
1	83.40	890	2.660	104.00	1224	2.560	125.80	1720	2.480
1.5	50.50	685	2.660	63.10	921	2.560	74.00	1234	2.480
2	17.60	480	2.700	21.20	620	2.570	22.20	760	2.490
2.5	3.30	345	2.750	1.40	511	2.640	0	705	2.555
3	- 1.60	200	2.850	-1.10	400	2.710	-1.1	650	2.625
3.5	- 6.50	60	2.950	-3.60	300	2.780	-2.2	600	2.695
4	-11.40	0	3.050	-6.10	200	2.850	-3.3	550	2.765

$10 \log \frac{U\theta}{\nu}_{crit}$	f = 10 $\frac{\beta_r \nu}{U^2} = 2.5\ 10^{-4}$			f = 11 $\frac{\beta_r \nu}{U^2} = 5.10^{-4}$			f = 12 $\frac{\beta_r \nu}{U^2} = 7.5\ 10^{-4}$		
	T_o	K_1	K_2	T_o	K_1	K_2	T_o	K_1	K_2
1	182.00	3025	2.240	218.80	4215	2.040	213	4930	1.945
1.5	100.50	1965	2.240	111.40	2670	2.040	104.5	3120	1.945
2	19.00	880	2.240	4.00	1800	2.040	-4	1330	1.945
2.5	-7.70	845	2.400	-103.40	1045	2.040	-4	0	1.945
3	-7.70	810	2.560	-103.40	200	2.040	-4	0	1.945
3.5	-7.70	770	2.720	-103.40	0	2.040	-4	0	1.945
4	-7.70	730	2.880	-103.40	0	2.040	-4	0	1.945

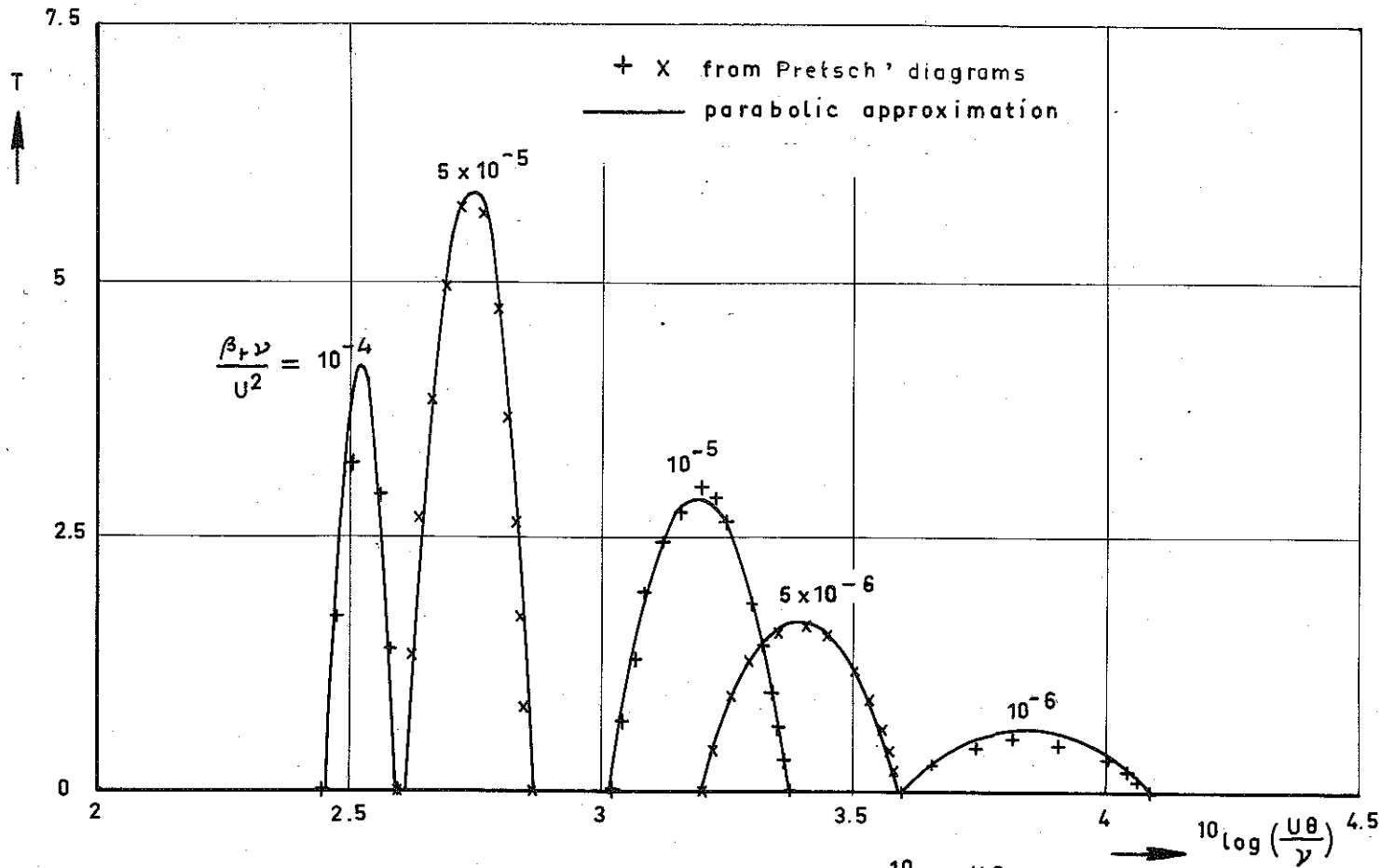

FIG. 1 : THE FUNCTION T FOR $\beta = 0$ AS FUNCTION OF $^{10}\log \frac{U\theta}{\nu}$

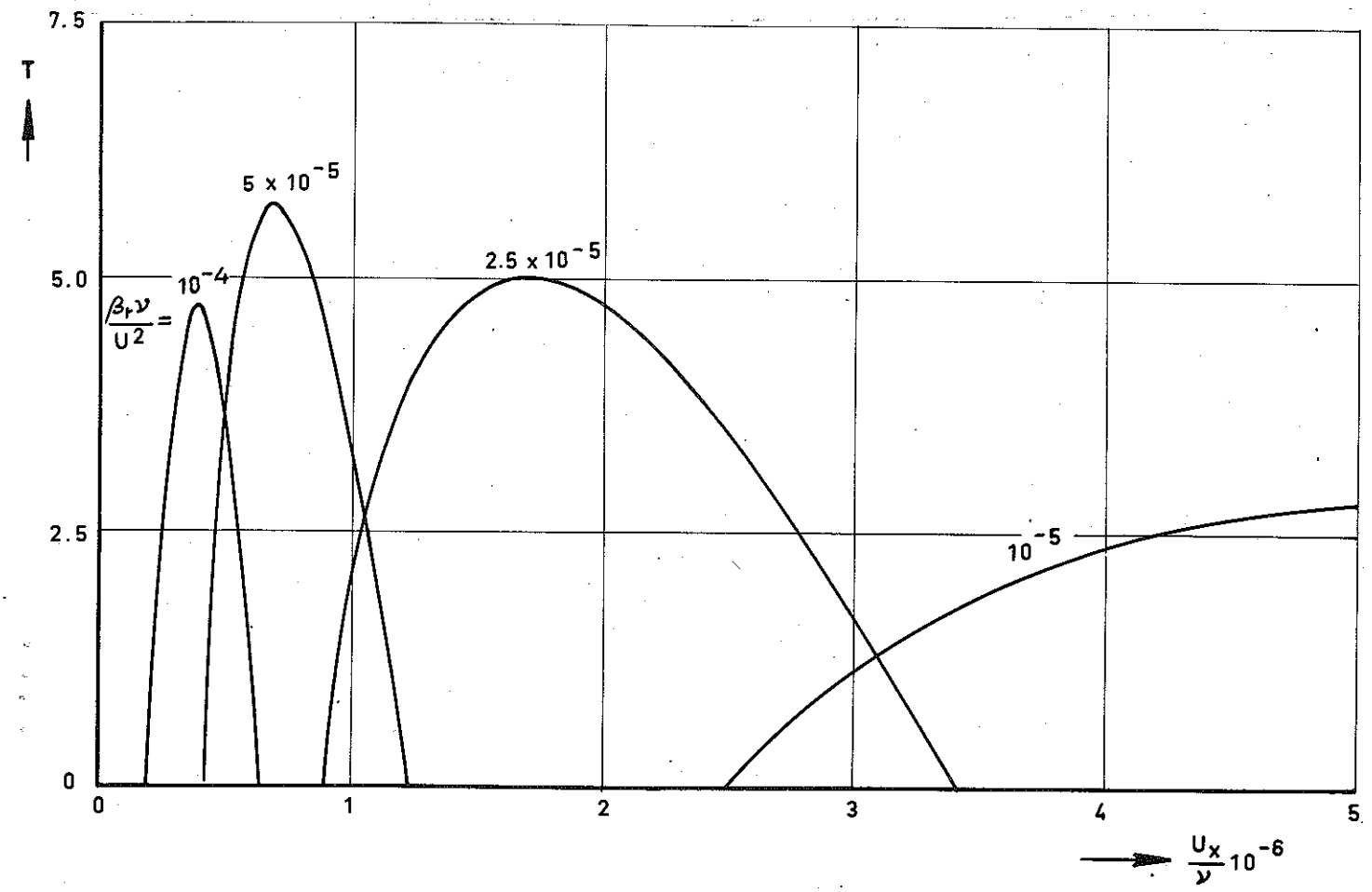

FIG. 2 : AMPLIFICATION RATE T FOR THE FLAT PLATE ($\beta = 0$)

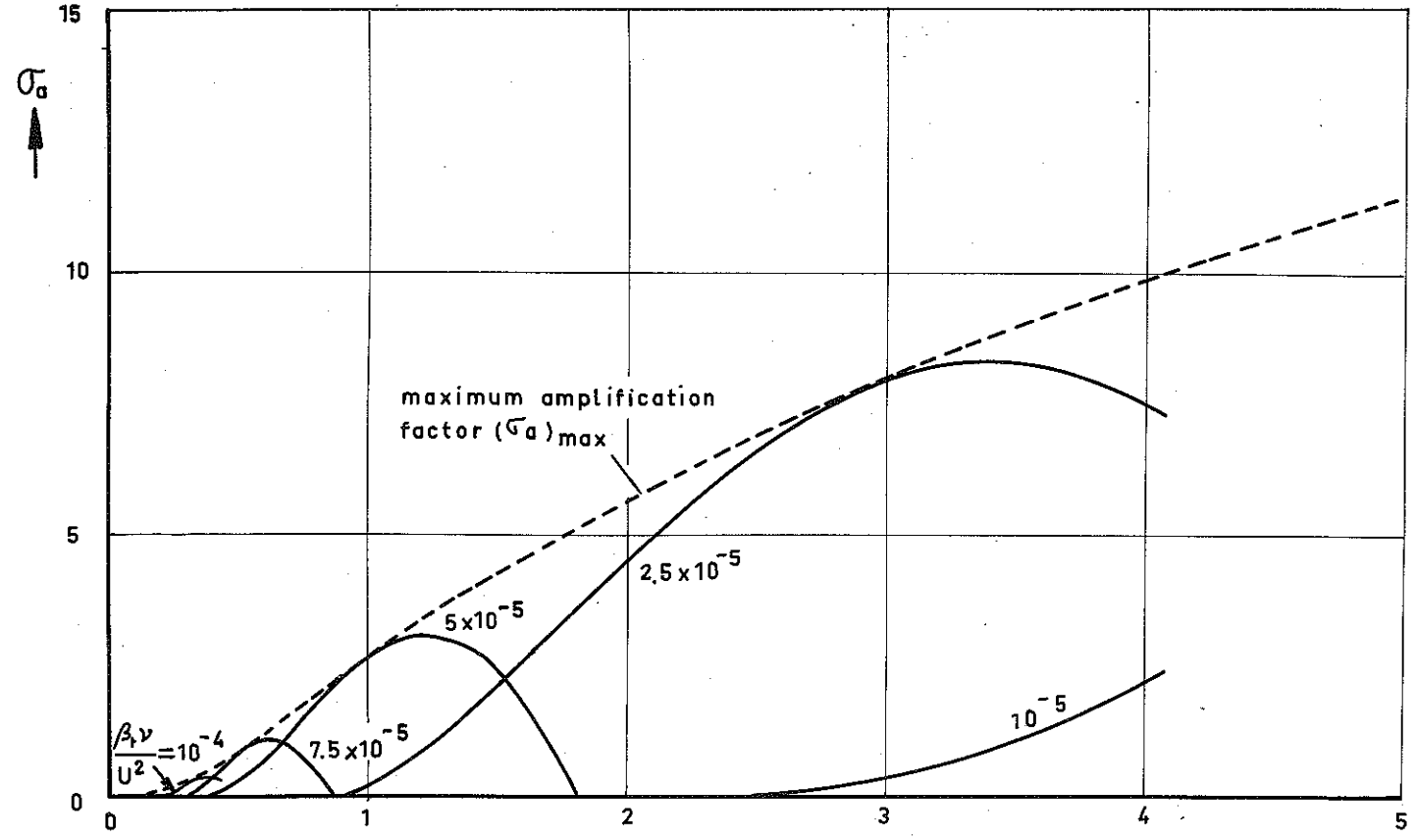

FIG. 3 : AMPLIFICATION FACTOR σ_a FOR THE FLAT PLATE ($\beta = 0$)

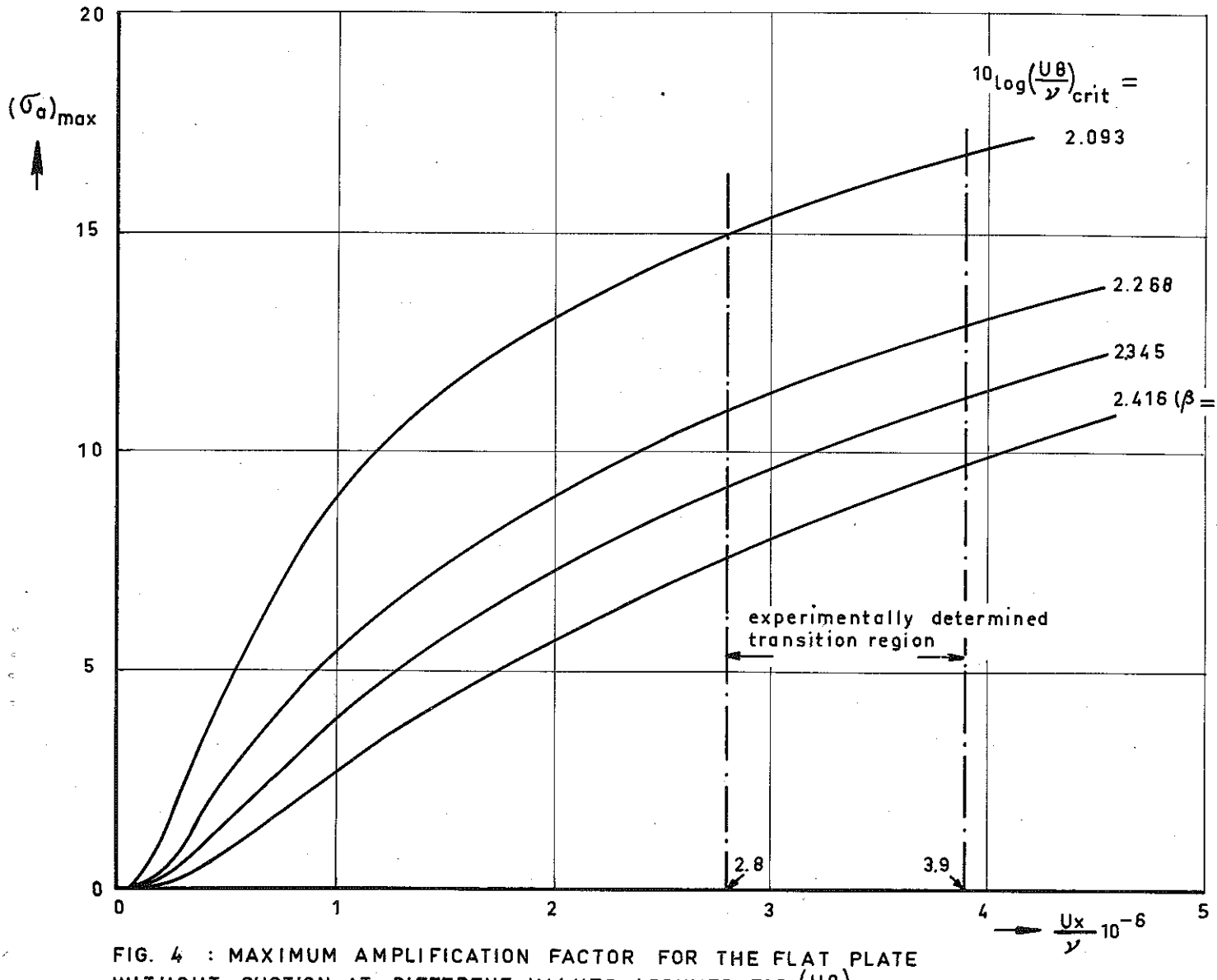

FIG. 4 : MAXIMUM AMPLIFICATION FACTOR FOR THE FLAT PLATE WITHOUT SUCTION AT DIFFERENT VALUES ASSUMED FOR $\left(\frac{U\theta}{\nu}\right)_{crit.}$

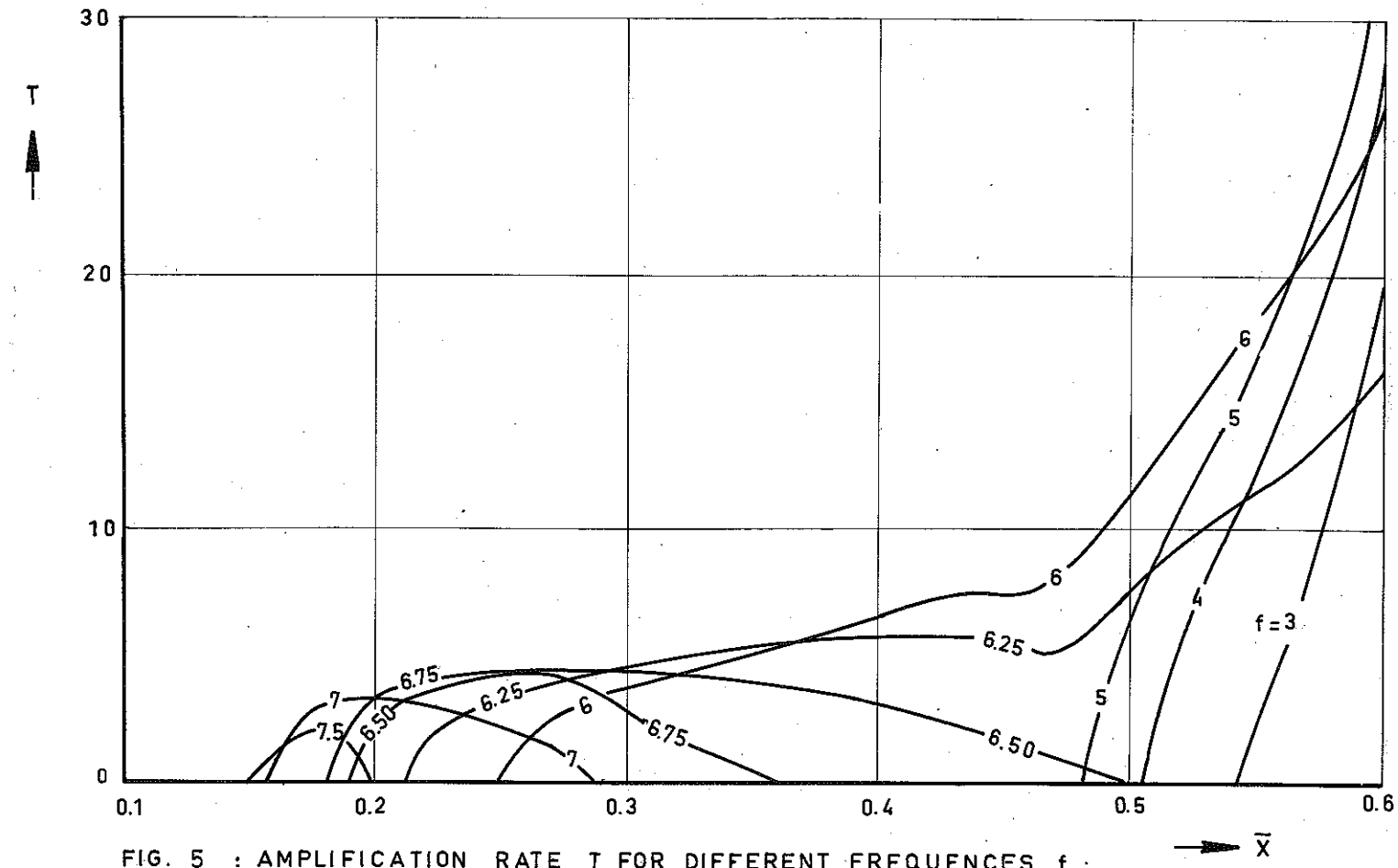

FIG. 5 : AMPLIFICATION RATE T FOR DIFFERENT FREQUENCES f ;
EC 1440 AIRFOIL SECTION ; $\alpha = 0$, $R_c = 4.35 \times 10^6$.

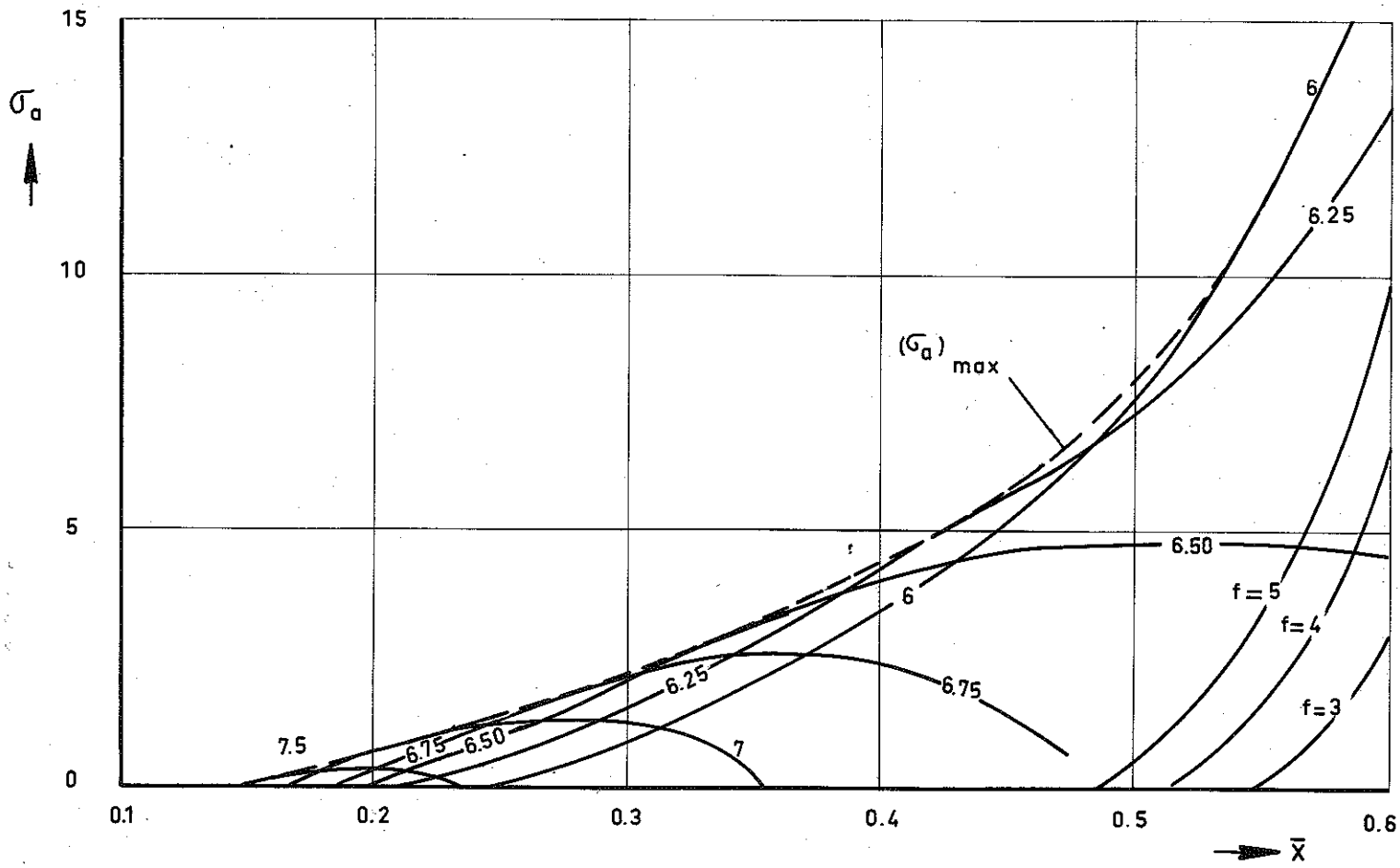

FIG. 6 : AMPLIFICATION FACTOR FOR DIFFERENT FREQUENCES f ;
EC 1440 AIRFOIL SECTION ; $\alpha = 0$, $R_c = 4.35 \times 10^6$.

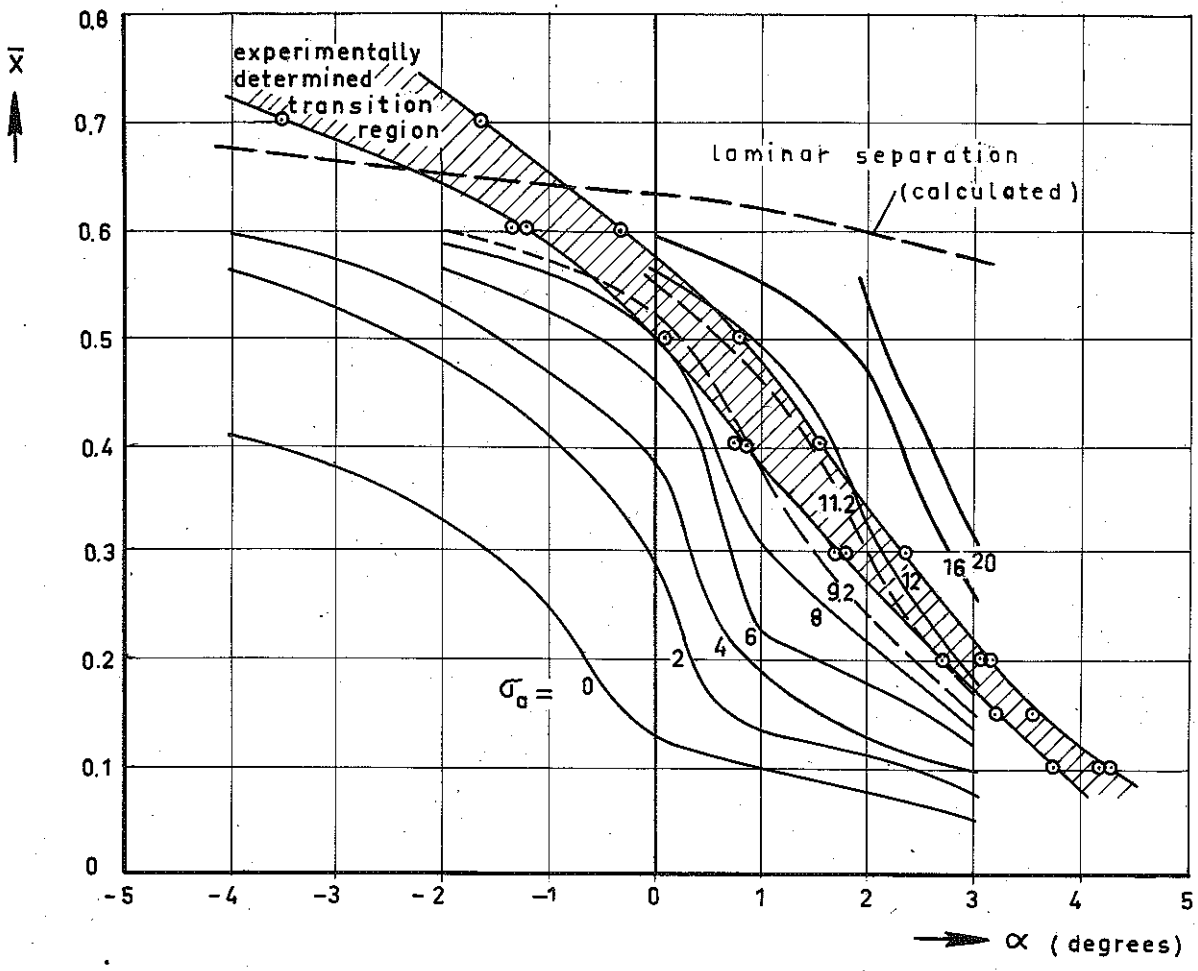

FIG. 7 : CALCULATED AMPLIFICATION FACTOR AND MEASURED TRANSITION REGION FOR THE EC 1440 AIRFOIL SECTION.

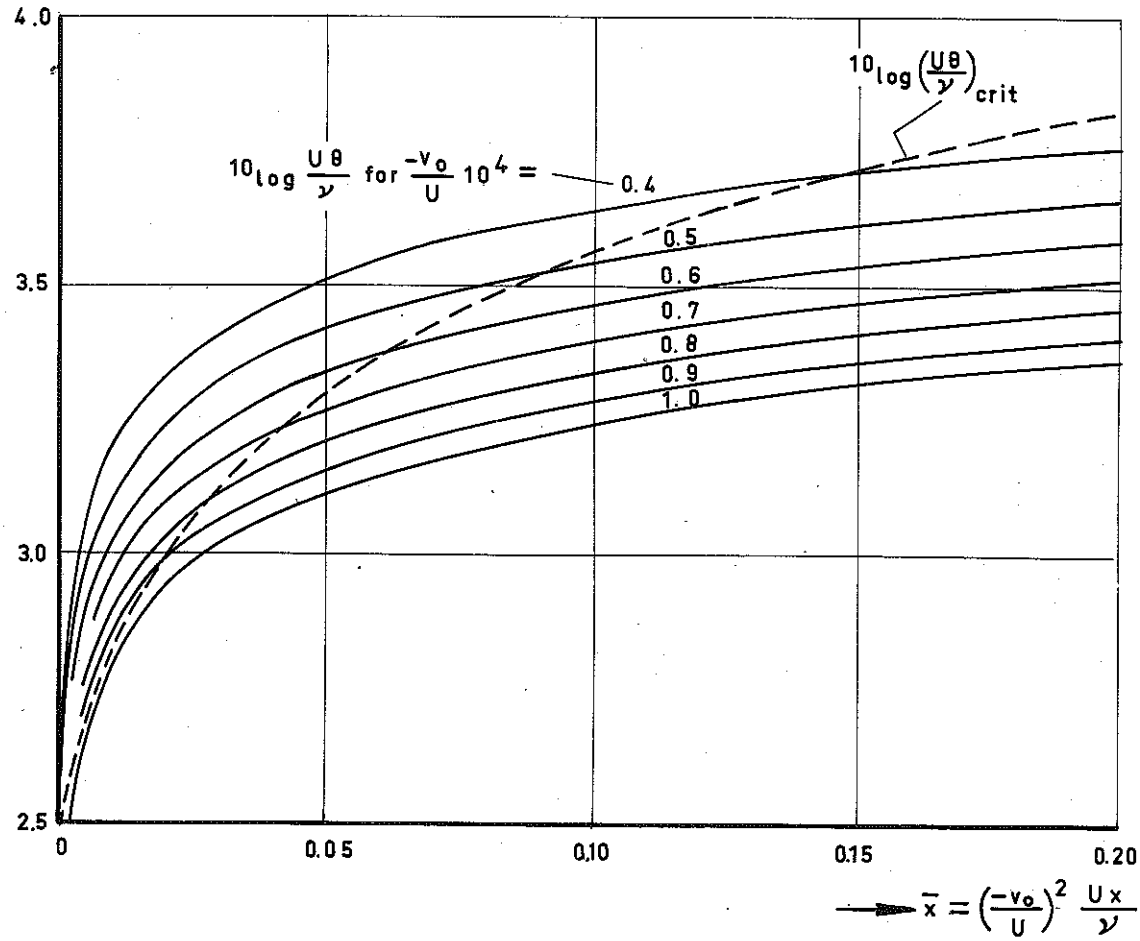

FIG. 8 : FLAT PLATE WITH CONSTANT SUCTION VELOCITY: $10\log\left(\frac{U\theta}{\nu}\right)_{crit}$ AND $10\log\frac{U\theta}{\nu}$ FOR DIFFERENT SUCTION COEFFICIENTS.

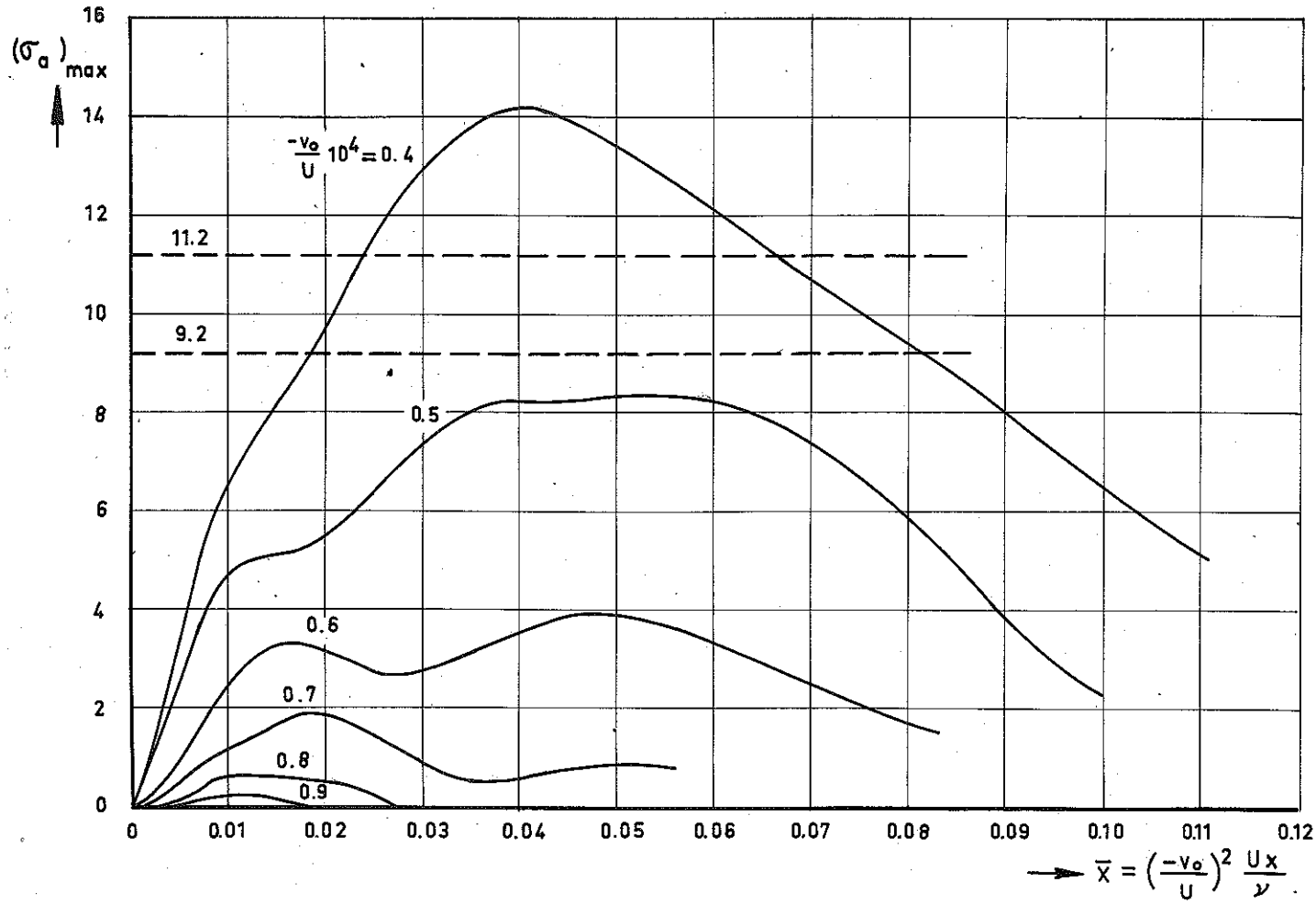

FIG. 9 : MAXIMUM AMPLIFICATION FACTOR FOR THE FLAT PLATE WITH CONSTANT SUCTION VELOCITY AT DIFFERENT SUCTION FLOW COEFFICIENTS.

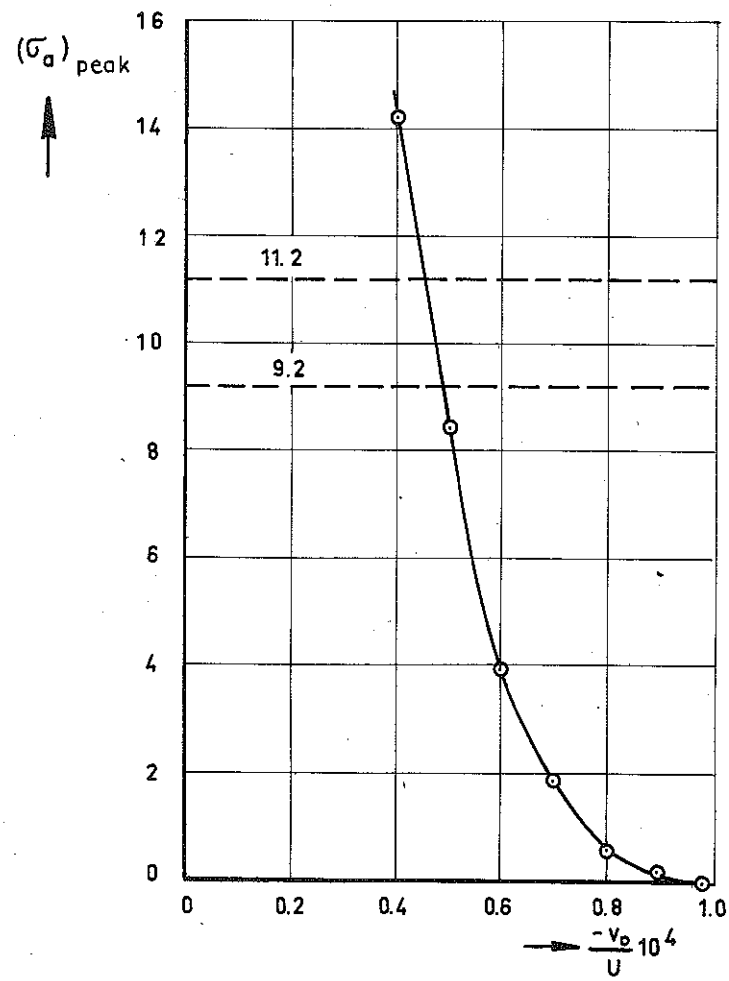

FIG. 10 : CROSS PLOT FROM FIG.9 ; PEAK AMPLIFICATION FACTOR FOR THE FLAT PLATE WITH CONSTANT SUCTION VELOCITY.

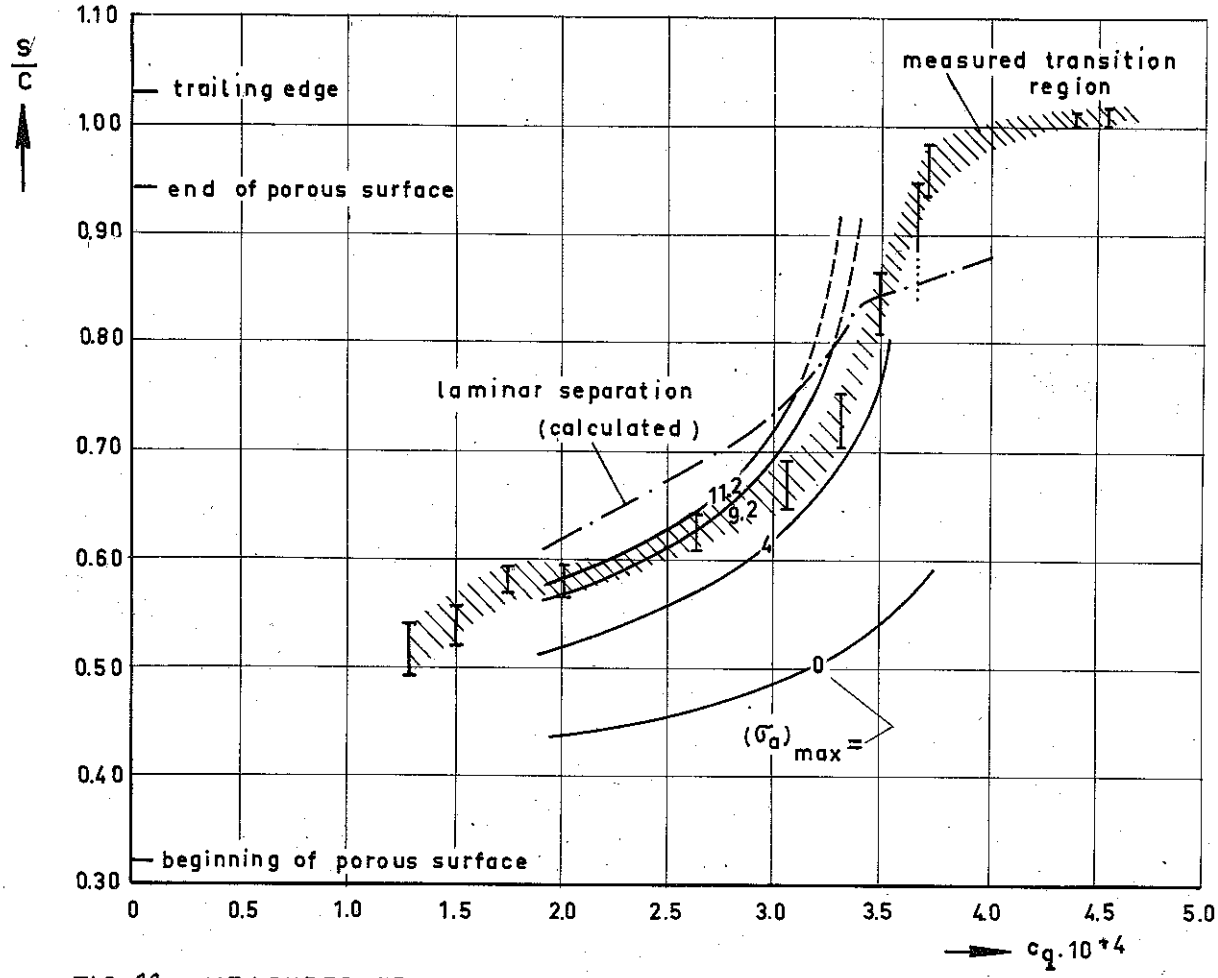

FIG. 11 : MEASURED TRANSITION AND CALCULATED AMPLIFICATION FACTOR FOR THE UPPER SURFACE OF THE SUCTION MODEL, $\alpha = 0°$, $R_c = 3.37 \times 10^6$

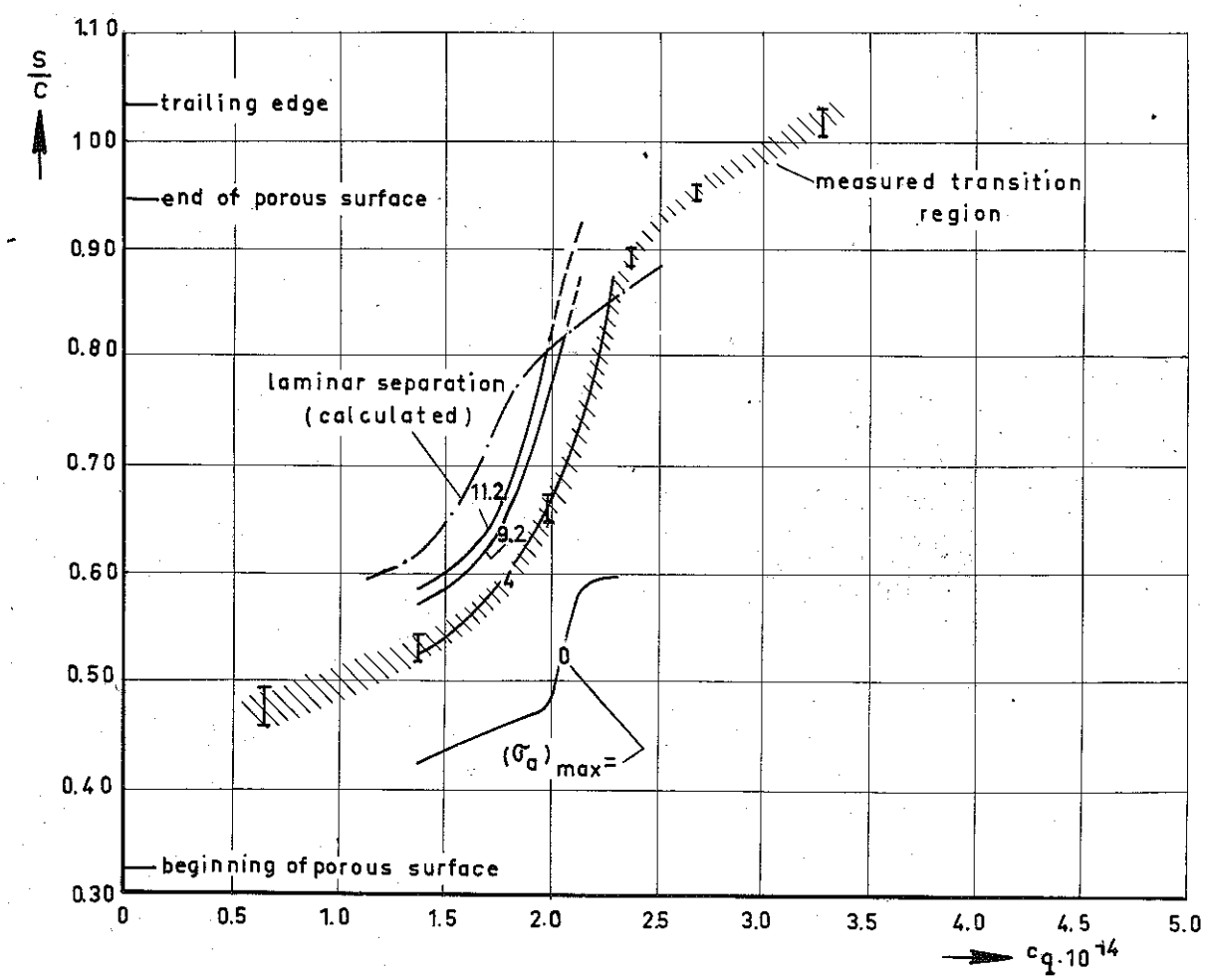

FIG. 12 : MEASURED TRANSITION AND CALCULATED AMPLIFICATION FACTOR FOR THE UPPER SURFACE OF THE SUCTION MODEL ; $\alpha = 0°$, $R_c = 6.16 \times 10^6$.